Local Luminance Nonlinearity and Receptor Aliasing in the Detection of High Frequency Gratings

Sheng He* and Donald I. A. MacLeod
Department of Psychology, University of California at San Diego, La Jolla, CA 92093-0109

Contrast sensitivity for orientation discrimination is limited to spatial frequencies below 50-60 cycles per degree by neural spatial integration, and we find that contrast sensitivity, measured using an orientation discrimination criterion, declines sharply with increasing spatial frequencies in that range. Yet interference fringe patterns pulsed at constant mean luminance can be detected at spatial frequencies far above that resolution limit [Williams, *Vision Research*, 25, 195 (1985)]. This is due at least in part to aliasing by the receptor mosaic, but another possible cue is provided by nonlinear distortion, which can create spatially uniform temporal transients when a pulsed fringe pattern is presented. We have investigated the contribution of these spatially unstructured distortion products to grating detection by superimposing the pulsed fringe patterns on a randomly flickering uniform field. This manipulation has almost no effect on contrast sensitivity well below the resolution limit. Just above the resolution limit, however, the random luminance mask greatly elevates the fringe pattern detection threshold, suggesting that spatially unstructured cues provide the basis for detection in this range. At still higher fringe pattern frequencies, that approximately match the cone mosaic, the random luminance flicker again becomes ineffective for some observers. This creates, in some observers, a clear secondary peak in contrast sensitivity in the flicker mask condition, presumably due to spatially structured cues provided by aliasing with the cone mosaic. The aliasing peak is still more clearly demarcated if the subject sets contrast thresholds for the perception of pattern as such. The contrast sensitivity function (CSF) then has a notch or gap between the normal sensitivity range and the aliasing range. Apparently in the unmasked case, spatially uniform cues (changes in overall color and brightness) bridge this gap.

1. INTRODUCTION

With a laser interferometer, interference fringe patterns (grating patterns with sinusoidal intensity profiles) can be generated directly on the observer's retina, bypassing the diffraction at the pupil aperture that limits the contrast of fine patterns in ordinary viewing. This makes it possible to isolate and investigate the extent to which visual resolution is limited by neural factors (such as the extent to which visual resolution is limited by size of the photoreceptor cells and the extent of spatial integration within the receptive fields of postreceptoral neurons), as opposed to optical factors. If the spatial frequency (lines per degree of visual angle) of this grating pattern is lower than the resolution limit, stripes are visible. If the spatial frequency is higher than the resolution limit, the stripes themselves will not be visible, by definition; but the fringe pattern may still be discriminable from a physically uniform field. The subjective manifestations of an unresolved interference fringe pattern, interpolated into a uniform field of the same space average intensity are complex. The field may change in brightness or color, it may appear to shimmer with quasi-random flicker, and it may show a fine but aperiodic spatial structure [1-3]. The last phenomenon has been convincingly shown to result from aliasing with the receptor mosaic [3]. Figure 1 illustrates the aliasing phenomenon for the case of a sinusoidal grating. Aliasing occurs because the visual receptors sample only discrete points in space. Figure 1 shows how two sinusoidal gratings of different frequency may be aliases of each other for the receptor array shown under the grating patterns, in the sense that they produce identical stimulation of the array of receptors. A grating too high in spatial frequency to be resolved as such may nevertheless appear to the subject in the guise of a much lower-frequency alias, if the spacing of its light bars is approximately matched to the spacing of the cone photoreceptors in the retinal mosaic. So gratings finer

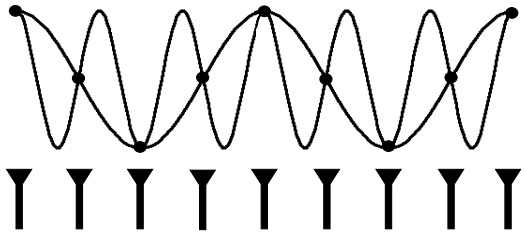

Figure 1. An array of receptors samples two sinusoidal gratings that are aliases of each other for this array. (After Williams, 1986)

than the resolution limit may be detected because they are aliased into much lower frequencies, even though the irregularity of the human receptor mosaic makes the aliases of very fine gratings wavy and distorted (the "zebra stripes" of Williams[3]).

For the origin of the flicker and of the alteration of color and brightness, a plausible hypothesis is that these are due to a local compressive or expansive nonlinearity[4,5]. When a pattern is not resolvable, such a nonlinearity may nevertheless make it detectable, because the uniform response to the unresolved pattern, formed by spatial integration of the nonlinear local responses, will be less or more than the response to a truly uniform stimulus. In a linear system, we can keep the average output level constant if the average luminance level is constant at the input. When fringe pattern contrast is modulated by adding and taking away the same amount of light in the bright and dim bars respectively, the mean output will not change. For a nonlinear system, the situation is different. We have demonstrated a local compressive nonlinear mechanism underlying the phenomenon we call contrast-modulation flicker [6]. Figure 2 illustrates the behavior of a compressive nonlinear mechanism. When the input contrast is zero (i.e., an uniform input), both input and output are spatially uniform (thick solid lines in Figure 2). When the fringe pattern has high contrast, the input intensity is increased in the bright bars and decreased by the same amount in the dim bars; but in the nonlinearly compressed output, the amount added in the light bars is less than that being subtracted from the dark bars. The net effect when the fringe pattern comes on is an overall reduction in space average output (thick dashed line in Figure 2). This could be visible as a uniform dimming of the field even if resolution losses later in the system obliterate the spatial fine structure of the fringe pattern.

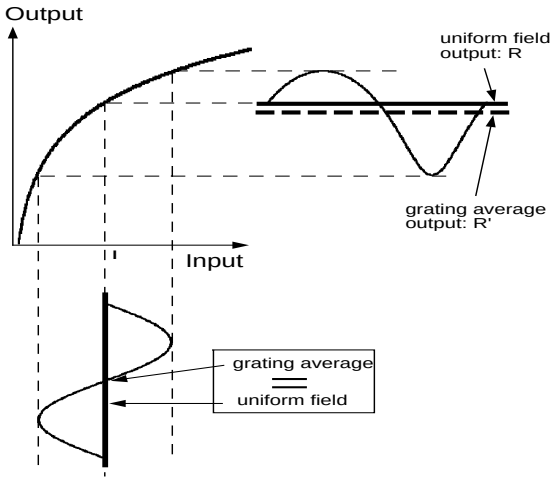

Figure 2. The effect of a compressive nonlinear transformation on a sinusoidal input. When the input is a uniform field with intensity I, the uniform output has the value R. When the input is a sinusoidal grating (with mean luminance I), the output is a distorted version of the sine wave. The effect of the added light in the bright bars is less than the effect of dimming the dim bars, thus, the mean output R' is less than R.

Detection of a fringe pattern briefly pulsed at constant space-average luminance might therefore be traceable to a spatially unstructured transient in apparent luminance or color generated by nonlinear distortion. If the duration of the fringe pattern is not negligible, the situation is complicated by the continuous occurrence of involuntary small amplitude eye movements [7]. These eye movements create random-polarity transients in local excitation when a fine fringe pattern is present. If these transients is nonlinear, the uniform output of the visual system derived by spatially integrating them will fluctuate, depending on whether the point of regard is momentarily almost stationary or moving relatively fast, since in the latter case the effective contrast of the pattern (and the magnitude of the local transients) will be reduced by temporal integration within the visual system. This is a likely cause of the observed flickering or shimmering of unresolvable fringe patterns, which provides a further spatially unstructured indication that a fringe pattern is present.

In principle, then, fringe patterns could be detected by any of three types of signal: (1) by direct resolution if the fringe pattern is not too fine to be resolved; (2) by perception of a spatial pattern that has been generated by aliasing with the receptor mosaic; and (3) by spatially unstructured cues (changes of overall color and brightness) such as those generated by nonlinear distortion during presentation of the fringe pattern.

In this paper, we will describe experiments designed to elucidate the role of each of these types of signal in the detection of very fine pulsed grating patterns. The results indicate that aliasing and nonlinear distortion are both important.

2. GENERAL METHOD

This section will describe the overall setup of the laser interferometer constructed for this research and the control of spatial frequency and contrast of the interference fringe pattern produced.

A. Apparatus

All the experiments reported here were done with a laser interferometer recently constructed at UCSD. It has 6 channels in all, but only the three beams diagrammed in Figure 3 were used in the present experiments. Beamsplitter, BS1, splits light from a Helium-Neon laser into two beams. Beam 1 was used to generate the fringe pattern, beam 2 served as a uniform equiluminous surround after passing through a diffuser. Beam 1 then goes through a acousto-optic modulator (AOM1), which is involved in the control of fringe pattern contrast as explained below. The spatial filter, SF, consisting of a microscope objective followed by a pinhole, expands the beam and removes spatial noise from it. Lens L1 collimates the expanded beam. Beam splitter BS2 splits the beam into two, each of the two resulting beams is then gated by double pass through a fast ferro-electric liquid crystal shutter (Displaytech, Boulder, Colorado), LCS1 and LCS2 respectively, which controls the contrast of the fringe pattern together with AOM as shown in next section. The double pass provides efficient extinction (to better than 10^{-5}), and this is necessary for effective control of fringe pattern contrast. After passing through a negative lens (L2 or L2'), each beam is reflected at a concave mirror (M2 or M2') and comes back through roughly the same path. L2, L2', M2, and M2' control the spatial frequency of the

fringe pattern by introducing small angular deviations into the returning beams in a fashion shown in next section. The two returning beams are recombined by BS2, then form a point image at position FS1 after passing through the positive lens L3. An adjustable stop conjugate with the pupil at FS1 is helpful in reducing stray light.(Correcting lenses can also be placed at this point, but none were necessary in these experiments) After FS1, the expanded beams are collimated again by lens L4. A circular field stop FS2, conjugate with the mirrors (M1 and M2) and with the retina, limits the spatial extent of the grating field on the subject's field of view. This was set for a diameter of 50 minutes of arc visual angle. Beam splitter BS3 combines the coherent beams with the incoherent beam, beam 2, used as the background in our experiments, and then L5 brings the beams to a focus near the cornea of the observer's eye.

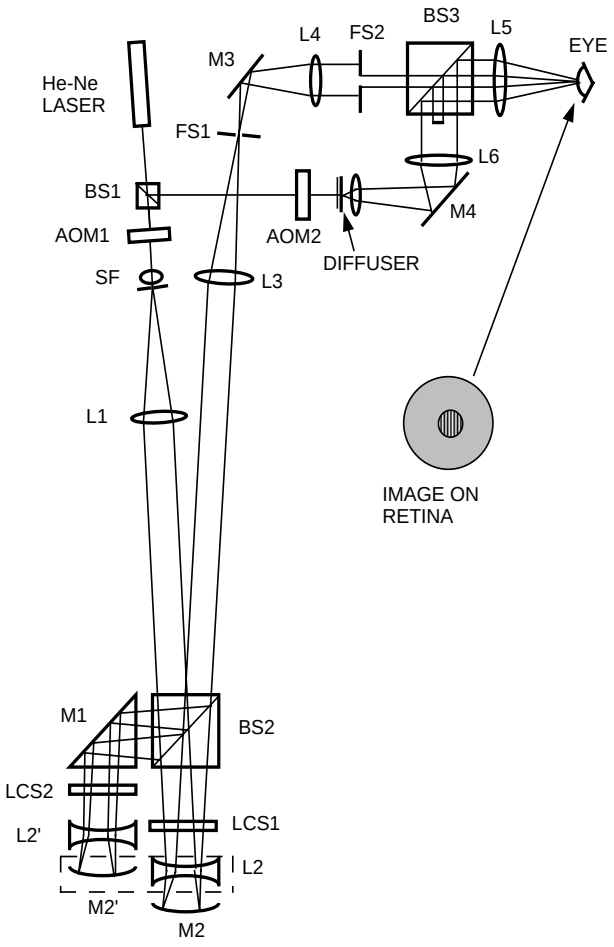

Figure 3. Schematic diagram of the laser interferometer, with inset showing subject's field of view. See text for details.

The inset shows what was usually seen by the observer. It should be noted, however, that under many conditions the fringe pattern present in the central field is not subjectively resolvable, and also that fields described here as "uniform" actually contained some random fine texture, rather like the speckle seen when laser light is reflected from a surface that is not perfectly smooth. In this case there is no such surface in the optical path before the eye, most of the speckle probably arises from fine scale inhomogeneities in the first surface of the cornea, though other refractive index variations probably contribute as well[8].

B. Spatial Frequency and Contrast Control

Both spatial frequency and contrast of the fringe pattern were controlled by a computer. In Figure 3, M2' and L2 are fixed on the same movable stage, driven by stepping motors (Nanomover, Melles-Griot) so that they can move together in any direction on the plane perpendicular to the optical axis. Movement of the stage results in symmetrical movement of the two returning beams (converging or diverging), as shown in Figure 4, thereby causing the two point source images in the observer's pupil to move symmetrically about the pupil center. With a given stimulus wavelength l, the distance a between these two points determines the spatial frequency of the fringe pattern n:

$$n \text{ (cycles/rad)} = a \text{ (mm)} / l \text{ (mm)} \qquad (1)$$

and their relative direction determines the fringe pattern orientation[3,9]. For the He-Ne laser, which has 632.8nm wavelength, the spatial frequency corresponding to a 1mm light separation at entrance pupil is 27.6 cycles/degree.

A critical point for these experiments is that when the contrast of the fringe pattern was modulated temporally, there should be negligible physical change in mean space-average luminance for each of the beams involved. This was achieved by the cooperation of LCS1, LCS2 and AOM1, using a technique essentially similar to that of Williams[3]: the two coherent beams are modulated very rapidly, and contrast is regulated by varying their overlap in time. Consider Figure 5. During each successive 3 msec, LCS1 was open for the first 2 msec whereas LCS2 was open for the last 2 msec, so creation of a fringe pattern was only possible during the middle millisecond when both shutters were open simultaneously. The fast acousto-optic modulator AOM1 placed in series with both LCS1 and LCS2, was opened for a time t1 during the middle millisecond, and t2 during each of the first and third milliseconds (see Figure 4). In this way, the contrast of the fringe pattern was equal to the ratio t1/(t1+t2), while the time average luminance for each beam was determined by the duration t1+t2; so by keeping the sum t1+t2=c constant, and varying the relative length of t1 and t2, we were able to modulate the fringe pattern contrast without varying the time averaged luminance of either beam. For example, when t1=p, t2=0, we obtained the maximum contrast, when t2=p, t1=0, we got zero contrast. Limited by the computer clock, t1 and t2 could be varied in steps of 0.2 usec. Rise times for the LCS and AOM shutters were 50 usec and 0.01 usec respectively. We checked the time average luminance with a photocell and wave analyzer, and found that when the fringe pattern contrast was modulated sinusoidally from 0 to 100%, the artifactual luminance signal generated was only 0.4%.

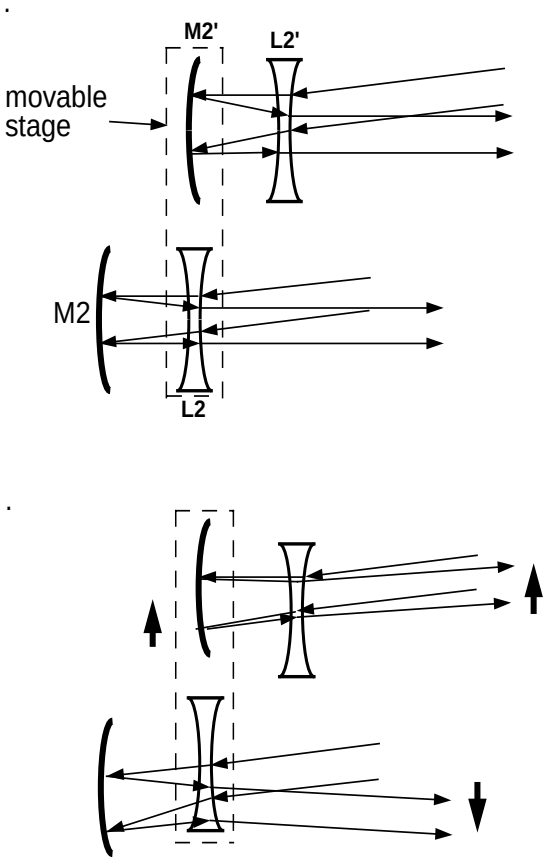

Figure 4. Control of fringe pattern spatial frequency. L2 and M2' are fixed on a stage which can be moved in any direction perpendicular to the optical axis. a) Stage in its zero position, generating zero spatial frequency fringe pattern (uniform field); b) when the stage moves in the direction shown, the two returning beams move apart in opposite directions symmetrically, they then form point source images symmetrical about the center of the pupil of the observer's eye.

In the first experiment, we measure forced-choice contrast thresholds for orientation discrimination, in order to define the limits of resolution without benefit from aliasing or from spatially unstructured cues. In the second experiment we make the spatially unstructured cues less visible by introducing random perturbations of the field luminance when the fringe pattern is presented. The aim here is to define the conditions for detection of pattern as such, including both resolution of the individual stripes below the resolution limit and detection of relatively low-frequency alias patterns above it, without the intrusion of spatially uniform transients generated by nonlinear distortion.

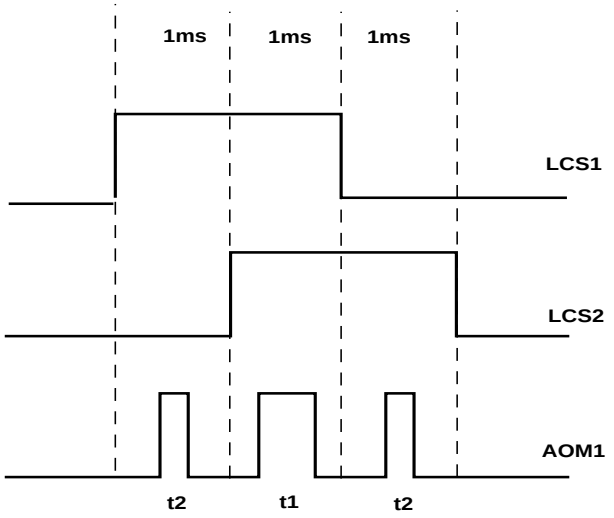

Figure 5. Fringe pattern contrast control. During each successive 3 msec, the shutters LCS1 and LCS2 are open for the first and last two msec respectively. The modulator AOM is opened to supply both beams for t1 during the second msec, and t2 for the first and third msec. Fringe pattern contrast is determined by the ratio t1/(t1+t2). The total open time for each beam is t1+t2 and this is held constant during the presentation of the fringe pattern.

3. EXPERIMENT 1: DETECTION BASED ON DIRECT RESOLUTION OF FRINGE PATTERNS: ORIENTATION DISCRIMINATION

With the use of interference fringe pattern stimuli, high contrast gratings can be generated on the observer's retina at arbitrarily high spatial frequencies. If the spatial frequency is higher than about 60 cpd, the pattern of alternating light and dark bars is not subjectively resolvable as such [2]. Surprisingly, however, subjects can successfully detect pulsed fringe patterns with high spatial frequencies as high as 200 cpd [3]. Williams used a two interval forced choice psychophysical procedure to measure the contrast sensitivity, while previous researchers used subjective assessments of pattern visibility. As mentioned above, there are a number of cues that a subject might, in principle, use to detect the presence of high spatial frequency fringe patterns. We want to know: what will the CSF look like if we use the forced choice procedure, yet the subject's response can only be based on direct resolution of gratings themselves? In other words, we wish to investigate the human resolution limit for fringe patterns objectively with a forced choice procedure. One good way to eliminate cues other than the direct resolution of fringe patterns is to ask subjects to discriminate between patterns of different orientation. Although aliasing could provide some gross orientation information[10], the orientation of the alias pattern is almost random and so it should not allow fine orientation discrimination.

A. Procedure

Contrast sensitivity for orientation discrimination was measured on 5 subjects. Thresholds were measured with a two alternative forced choice technique with feedback. On each trial, a 1000 msec interval was defined by two clicks from the computer which a fringe pattern was presented. A fringe pattern with space-average luminance I_m, spatial frequency f and rotated counterclockwise θ degrees has the intensity distribution:

$$I(x,y) = I_m \{1 + A \cos[2\pi f (x \sin\theta + y \cos\theta)]\} \qquad (2)$$

where x and y are the horizontal and vertical spatial coordinates in degrees within the stimulus field, and f is the spatial frequency in cycles per degree (cpd). A is the contrast of the fringe pattern, and is varied during the experiment to find the threshold level without change in I_m. In our discrimination task, the fringe pattern could be in one of two possible orientations, randomly selected by the computer. We tested horizontal vs. vertical orientation, +5 vs. - 5 or +10 vs. -10 degrees from horizontal, and +45 vs. - 45 degrees from horizontal (or vertical) orientation. The space-average luminance of the test field I_m was usually 1000 td and was kept the same when the contrast was reduced to zero in the interval between trials. After each trial subjects responded by pressing one of the two response keys, depending on which orientation (horizontal or vertical fringe pattern, clockwise or counter-clockwise) was perceived. Fringe pattern contrast varied from trial to trial in a multiple interleaved staircase sequence, and contrast threshold was defined as the value estimated, from a cumulative normal fit to the results of 100 trials for each spatial frequency, to yield 84% correct responses. After each trial, the point sources were moved back to the center position, this ensured that the faint sound generated by the motor movement was not a valid cue for subject's response. The stimulus was presented in a centrally fixated circular field with 5 degrees diameter.

B. Results and discussion

Figure 6 shows the CSF for two observers based on the forced choice orientation discrimination task. Open circles are for the horizontal vs. vertical discrimination, filled circles are for discrimination of smaller angular differences (+- 10^0 for SH, +-5^0 for DM), and open squares are for + - 45^0 discrimination. Data for + - 10^0 discrimination were also collected for the other three subjects; these are very similar to the two subjects' data shown in Figure 6 (filled circles). The resolution limit demonstrated using the +- 5^0 or 10^0 orientation discrimination is consistent with previous results found with non-forced choice measures[2,11]. The resolution limit for DM and for SH is just below 60 cpd. In both cases, however, there is a very rapid fall off around spatial frequency 40-60 cpd: contrast sensitivity varies inversely as the 5th power of spatial frequency in the range 45 cpd to 60 cpd, much as in the results of Sekiguchi et al [11]. For the other subjects the contrast sensitivity fell just as rapidly but the resolution limit was lower: from 45 cpd to 55 cpd.

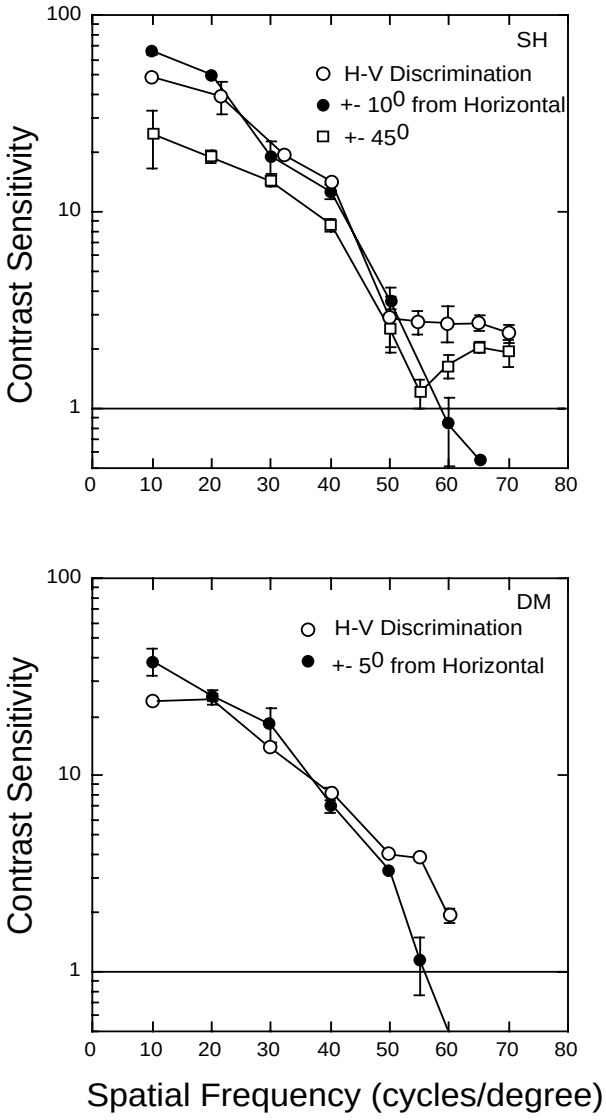

Figure 6. Contrast sensitivity (reciprocal threshold contrast) based on orientation discrimination for two observers. Open circles, horizontal vs. vertical grating discrimination; filled circles, smaller angular difference (+ 100 for SH, + 50 for DM) from horizontal orientation discrimination; open squares, + 450 from horizontal orientation discrimination.

In the case of discriminating horizontal vs. vertical, although we tried to eliminate cues other than orientation of the fringe pattern, it is hard to be certain that we really achieved this goal. Contrast thresholds for this coarse orientation discrimination were almost the same as for the fine discrimination up to 50 cpd, but at and above 50 cpd a "shoulder" appears in the coarse discrimination data, separating them from the fine discrimination data. This contrast sensitivity shoulder (more pronounced for SH than DM) at frequencies above 50 cpd is very likely supported by cues other than true pattern resolution. Near the resolution limit, the threshold contrast was considerably higher for vertical gratings than for horizontal ones of the

same frequency. This meridional variation in pattern sensitivity is interesting as evidence for different patterns of neural spatial integration (receptive field profiles) in orientation- selective cells of different preferred orientation, but it creates an experimental problem: because the staircase drove the vertical gratings to a higher contrast during the experimental measurement of threshold, aliasing patterns and unpatterned cues like brightness changes and desaturation, were more noticeable for vertical gratings than for horizontal gratings (especially for observer SH). This asymmetry of sensitivity to alias patterns or nonlinear distortion products from horizontal and vertical gratings provided one possible basis for discrimination.

A second possible cue is suggested by the observation of Sekiguchi et al.[12], who reported seeing "secondary zebra stripes" around the Nyquist frequency. These are thought to arise (most probably) from the same local nonlinear mechanism that generates the brightness distortion product, acting in conjunction with sampling by the cone mosaic. The sampled image of a grating near the Nyquist frequency has quite non-uniform contrast: in regions where its adjacent bright and dim bars happen to be aligned with adjacent rows of cones, adjacent cones will be exposed to very different light intensities, forming a pattern of high effective contrast; at the same time at a nearby retinal location, the same grating could have its bright and dim bars fall out of register with the cone mosaic, with the result that adjacent cones will be exposed to not very different light levels, hence low contrast. Even if the bright and dim bars are too fine to be resolved as such, this relatively coarse pattern of contrast variation acting on a locally nonlinear process like that of Figure 5 will give rise a perceptual brightness variation, the so called "secondary zebra stripes". Subject SH reported seeing such "secondary zebra stripes" within a small area in the central fovea, as a semi-randomly oriented set of relatively coarse stripes in the frequency range 50-70 cpd when the contrast was about 60% or above. This conceivably could support discrimination for gross (horizontal vs. vertical or $+-45^0$) orientation differences (more about this in the general discussion) but not for small angular differences. In situations where the fine ($+-5^0$ or $+-10^0$) and coarse (horizontal vs. vertical or $+-45^0$) forced-choice thresholds disagree, it was only at or above the fine discrimination threshold that the subject experienced any distinct awareness of the pattern spatial frequency and orientation. This fact, and the agreement between the fine discrimination data and the self adjusted thresholds of other studies [2, 11] lead us to prefer the fine discrimination forced-choice thresholds as indices of pattern resolution.

If the coarse discrimination “shoulder” is discounted for the reasons mentioned, the fine discrimination forced-choice thresholds of Figure 6 show a precipitous loss of contrast sensitivity, varying inversely approximately as the fifth power of spatial frequency, at spatial frequencies around 50 cpd. Like the self-adjusted thresholds of Campbell & Green[2] and Sekiguchi et al [11], these data clearly indicate significant postreceptoral neural limitations on contrast sensitivity, since spatial integration within the apertures of the cone receptors themselves has been shown to preserve pattern contrast up to approximately twice that spatial frequency [13].

Fringe patterns of 60 cpd or more did not allow fine orientation discrimination. This suggests that they are detected either through aliasing or through spatially unstructured products of nonlinear distortion. The following experiment was done to decide between these possibilities.

4. EXPERIMENT 2: FRINGE PATTERN DETECTION WITH AND WITHOUT RANDOM LUMINANCE MASKING

A regularly sampled fringe pattern has an alias of spatial frequency fa=fs-f, where fs is the spatial frequency corresponding to 1 cycle per cone spacing and f is the fringe pattern frequency. Assuming that 0.29mm on the retina corresponds to 1deg [14], fs is estimated to be about 110-120 cpd. [15, 16]. Based on these facts, we would expect that the sensitivity to aliasing patterns should be a mirror image of the conventional sensitivity, reflected about the Nyquist frequency, f/2 as shown in Figure 7. The mirror image prediction is not quite realistic, because the foveal cone mosaic shows a degree of irregularity [17]. This distributes alias energy over a range of spatial frequency, creating two-dimensional bandpass-filtered noise as the alias of a supra-Nyquist frequency fringe pattern. As we will show in the Discussion, this may reduce the height of the aliasing peak (to a degree depending on the bandwidth of the detecting mechanism), and broaden it, but it should not alter its bandpass character. The expected spectral broadening due to foveal sampling (very roughly +10 cpd based on Yellott's evidence[17]) is not very large, and the bandwidth of the neural visual system for two-dimensionally bandpass filtered spatially random patterns (such as the alias of a supra-Nyquist fringe pattern) is narrower still, narrower than the system’s bandwidth for gratings[18]. The net effect (see Discussion, and the dashed curve in Figure 10 below) is that the alias peak is theoretically expected to be about as sharp as the peak for direct resolution below the Nyquist frequency.

If the detection of fringe patterns is based on direct resolution at low spatial frequency and on aliasing patterns at high spatial frequency (as Williams [3] has suggested), we would therefore expect a CSF with a "notch" around the Nyquist frequency. Yet the results of Williams [3] show a monotonic decrease in sensitivity as spatial frequency increases.

In this experiment we address the possibility that it is the detection of nonlinear distortion products that fills in this theoretically expected notch. Because the nonlinear distortion would be expected to yield spatially unstructured changes in the field when the fringe pattern comes on (such as a subjective brightness change, quasi-random flicker during the presentation of the pattern, or a chromatic desaturation), we might be able to reduce its effectiveness as a cue by adding an uniform random luminance mask to the test field, while the direct resolution of the fringe pattern and its aliasing product will be largely unaffected. If our hypothesis is correct, this experiment might reveal the bimodal sensitivity distribution that we would expect if

aliasing alone is responsible for detection of fringe patterns above the resolution limit. Figure 8 shows the possible shape of CSF under two different conditions: with and without a random flicker masking background.

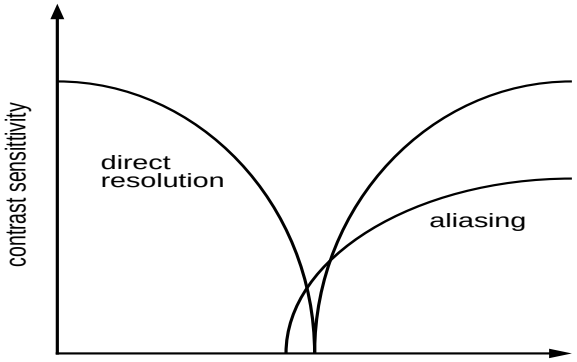

Figure 7. Schematic diagram of sensitivity to fringe patterns (when the spatial frequency is less than the Nyquist limit, about 55-60 cpd) and to aliases produced by interaction with a regular receptor mosaic (when the fringe pattern frequency is higher than Nyquist limit and up to about 110-120 cpd, the assumed sampling frequency of the mosaic). Lower curve shows sensitivity to aliases after taking receptor irregularity into consideration.

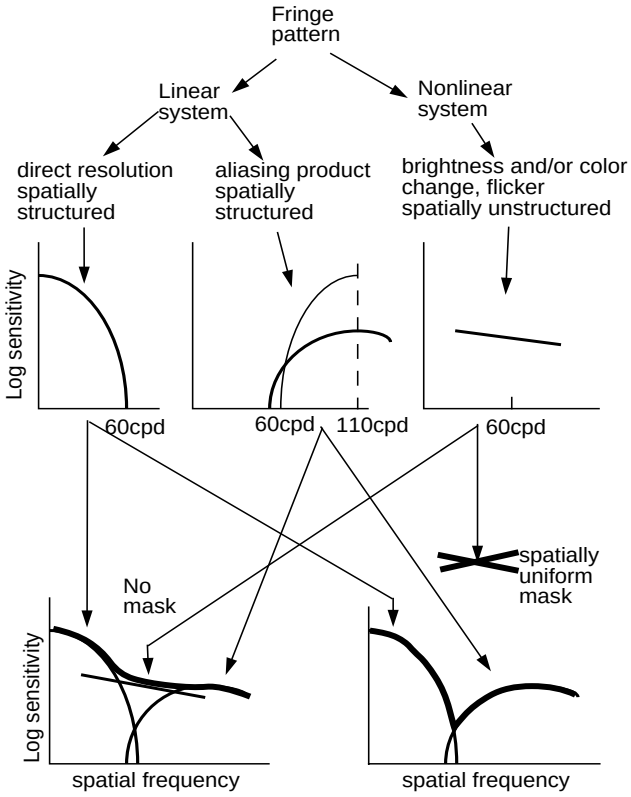

Figure 8. Rationale underlying experiment 2. A fringe pattern could be detected by any of the three types of signals: the fringe pattern itself, its spatially structured aliasing products and its spatially uniform nonlinear distortion products. A spatially uniform luminance mask should selectively reduce the effect of nonlinear distortion product as a detection cue, thereby exposing the two distinct sensitivity lobes associated with direct resolution and with aliasing.

A. Procedure

A two-alternative temporal forced choice procedure was again used. On each trial only one vertical fringe pattern was presented, and it appeared randomly in one or the other of the two intervals. During that interval the contrast of the fringe pattern was windowed by a truncated Gaussian function of time with a standard deviation of 157 msec. Subjects responded by pressing one of the two keys depending on which interval they thought that the fringe pattern appeared. Two observers participated in this experiment, with less complete checks on a third observer. The experiment was run under two conditions. In one condition, the mean luminance of the test field remained constant before, during and after presentation of the fringe pattern. This was similar to the procedure used by Williams[3]. In another condition, there were random luminance changes during each interval. These consisted of (1) a random shift of time average luminance, by a scaling factor with a rectangular distribution in the range 0.5 to 2, which was independently selected for each interval and was sustained for the duration of the interval, and (2) a random luminance flicker, produced by resetting the field luminance every 3 msec to a value between 0 and twice its time average; the luminance multipliers for successive 3 msec intervals were independent samples from a rectangular distribution spanning the range 0 to 2. Figure 9 shows schematically how the stimulus contrast and luminance was varied during a trial under the random luminance masking condition. In conditions without luminance masking, the upper curve depicting the luminance variation would be always a straight line.

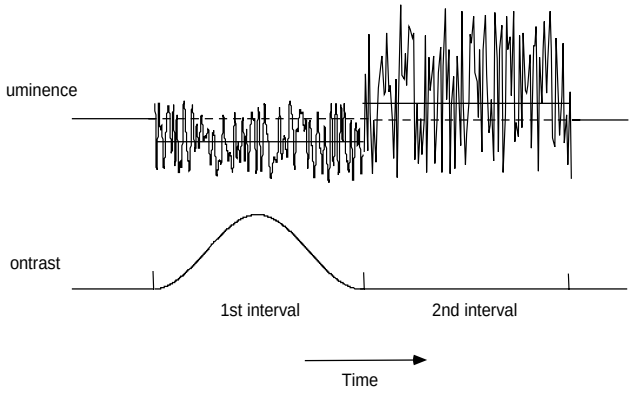

Figure 9. Stimulus waveform in the random luminance mask experiment. Upper curve shows the luminance masking noise randomly generated for each trial; lower curve shows the change of contrast in one of the two intervals. The subject must indicate in which interval the pattern appeared (here the first interval).

B. Results and discussion

Figure 10 shows the CSF of two observers under the two conditions. Standard errors are based on variation between the individual estimates from 3 different blocks of 100 trials each. The results we got without luminance masking

(open circles) are consistent with those of Williams: sensitivity declines almost monotonically with increasing spatial frequency. The CSF with the uniform luminance mask (filled circles), however, does show a clear notch. For observer SH, this notch is close to the resolution limit, which is in turn fairly close to the Nyquist frequency (two inter-cone spacings per cycle); for observer PD, the masking has a wider effective range above the resolution limit. In both cases, the uniform flickering mask greatly reduced sensitivity in intermediate spatial frequencies around and above the resolution limit, but the sensitivity was less affected by the uniform mask at both the low and high end of the spatial frequency range; here, detection was subjectively based on the explicit resolution and detection either of the fringe pattern stripes themselves (at low spatial frequencies) or of a spatially structured aliasing product (at very high spatial frequencies approaching twice the Nyquist frequency or twice the resolution limit). The difference between SH and PD is consistent with their subjective experience. SH experienced the "zebra stripe" like aliasing products described by Williams [3] just above the resolution limit, and these became a dominant cue for the appearance of the fringe pattern as the frequency went even higher. Observer PD did not see the "zebra stripe" aliasing pattern immediately above the resolution limit, but did see it at higher spatial frequencies; for this observer, aliasing became the dominant cue when the frequency went up to about 100 cpd. The third observer seldom saw aliasing at all.

Although the masking condition does expose a clear minimum in sensitivity (and a maximum in masking) in the neighborhood of the Nyquist frequency, it is not the deep and sharp notch theoretically expected. Our subjects did not see spatial structure at threshold at these spatial frequencies, but they did experience a color change: a desaturation of the field. This cue is presumably not much degraded when we add random luminance variation, and it could be the basis of the retained sensitivity. We tested this by giving up the forced choice procedure, and determining (by having the subject adjust the contrast of the pulsed fringe pattern with a trackball) the threshold needed for a subjective impression of spatial structure. The subjective pattern thresholds, taken together with the forced-choice orientation discrimination data at sub-Nyquist frequencies, do reveal the very distinct and narrow supra-Nyquist peak expected for aliasing (solid squares and open diamonds, Figure 10).

These results support the idea that under these conditions, and for these observers, a nonlinear distortion product is detected when a grating not too far above the resolution limit is at threshold, and that this distortion product is spatially uniform so that it can be masked by a spatially uniform random modulation of luminance. In addition, the distinct sensitivity peak (in the masking condition) for fringe patterns of still higher frequency, roughly matched in spatial period to the receptor mosaic is strong objective evidence that aliasing is the basis of observer's sensitivity to such high frequency fringe patterns. As discussed in the first experiment, the "secondary zebra stripes" [12] require a high fringe pattern contrast (about 60% or above) to be seen , and hence probably were not a factor in the present experiments.

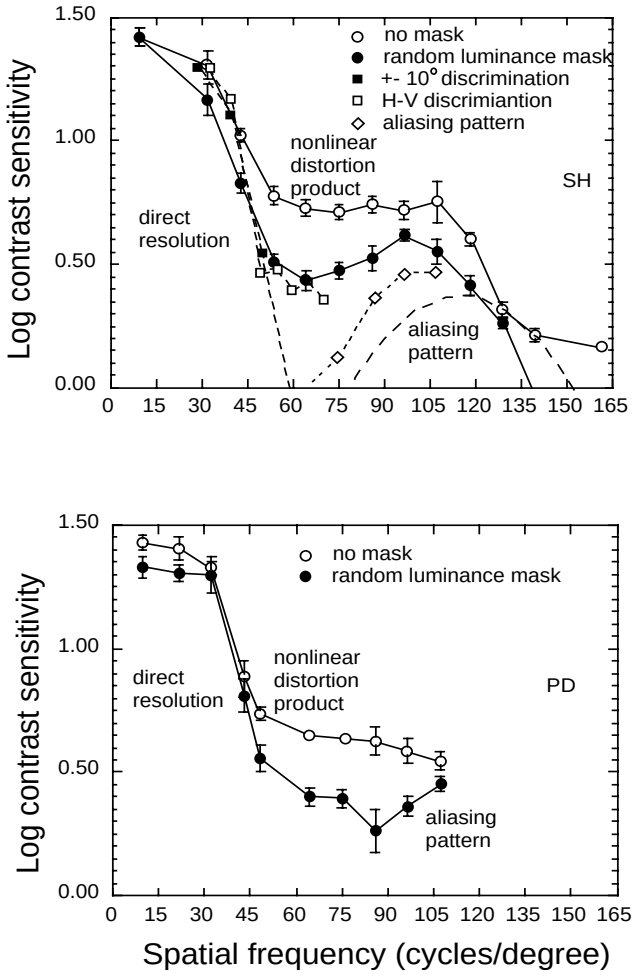

Figure 10. Results from experiment 2. Log contrast sensitivity for two observers as a function of spatial frequency, in two conditions: with random luminance mask (filled circles); and without random luminance mask (open circles). Error bars are plus and minus one standard error, based on variation between 3 estimates from different sessions with 100 trials each. For both observers, sensitivity was severely reduced by the uniform luminance mask for intermediate frequencies, but less affected at both low and high ends of the spatial frequency range. For SH, adjustment pattern sensitivities are shown as open diamonds, together with $+\text{-}10^0$ discrimination sensitivity (filled squares), it shows a deeper notch. The dashed curve represents predicted thresholds for pattern based on aliasing (see Discussion).

5. GENERAL DISCUSSION

A. Neural resolution limits (discrimination vs. detection)

The results of the first experiment show a precipitous loss of contrast sensitivity at spatial frequencies close to 60 cpd, presumably indicative of neural spatial integration in the detection of these fine patterns. The second experiment indicates that fringe patterns of spatial frequencies around 70 cpd, which did not allow orientation discrimination at

threshold, are detected by means of spatially unstructured cues created by nonlinear distortion, but that aliasing is critical for the detection of still finer fringe patterns that are roughly matched to the spatial period of the cone mosaic.

The interferometric CSF is usually identified with the neural CSF, because the effective contrast at the retina is almost free of optical loss [13]. There is a potential problem with this approach: as we have shown, the presentation of a pulsed high frequency fringe pattern could be detected through distortion products. This could give a falsely high estimation of the neural contrast-transfer function. Indeed, it has been generally found that detection of a pulsed grating has a substantial lower threshold than discrimination or resolution of a grating [3, 19, 20]. Even with an orientation discrimination task, angular difference plays a rather important role (Experiment 1 of this paper). If the angular difference is sufficiently large, the aliasing pattern could potentially support discrimination in two ways. 1). the aliasing pattern may contain more energy in the stimulus orientation than other orientations; 2). aliasing sensitivity may be different for different stimulus orientations. The fine discrimination task we used in our first experiment is a reasonable way to avoid this problem which, we think, gave a more realistic estimation of the neural CSF.

Thibos et al [21] found results similar to those of our Figure 6 (but at far lower spatial frequencies) with natural stimuli in peripheral vision. They suggest, however, that "the steep decline in contrast sensitivity for resolution just beyond the Nyquist frequency reflects a truncation imposed by neural sampling on the wider-ranging CSF for detection", whereas we interpret the decline in our foveal data in terms of neural filtering. The filtering interpretation appears plausible a priori, since it requires only that the detecting cells receive input from multiple photoreceptors, and this is certainly the case for orientation-selective cells, which have measurable misalignment of their cone inputs (Clay Reid, personal communication). The sampling interpretation has no such obvious basis: for a near-Nyquist frequency stimulus, the wide dispersion of aliased energy in the frequency domain (Figure 11) makes these Fourier components of the sampled stimulus weaker than the unaliased component, and it therefore seems unlikely that they would lead to confusion about the stimulus orientation. Indeed, irregular sampling imposes no absolute restriction at all on the spatial-frequency range of veridical grating perception, since orientation-selective receptive fields can always be extended (along their long axes) to create any desired one-dimensional sampling density! It is particularly difficult to imagine why sampling should lead to a very precipitous loss of orientation-discrimination contrast sensitivity at frequencies slightly below the Nyquist frequency, (as happens in our Figure 6), yet this is easily understandable if a neural spatial filter cuts off there. The orientation discrimination results of Thibos et al's Figure 5, which they regard as inconsistent with a filtering interpretation, are consistent with a neural filter having a steep high-frequency attenuation--just as we propose for the fovea, but perhaps as much as twice as steep.

A key observation in support of the neural spatial filter interpretation is the CSF "notch" exposed by our random luminance mask in Experiment 2. This is theoretically expected if there is a neural filter (see section B below), but is not readily explicable otherwise. As Figure 10 shows, the notch appears not just in orientation discrimination thresholds but also in subjectively set thresholds for seeing pattern. Even if there were a rationale for Nyquist-frequency "truncation" of the orientation-discrimination CSF by sampling, it presumably would not apply to these thresholds, which are for detection of any pattern and do not require veridical perception of orientation. Whatever may be the case outside the fovea, these observations indicate that the range of aliasing, by the criterion of subjective visibility of zebra stripes, does not extend down to the Nyquist frequency in the fovea. The visual system is sensitive only to low spatial frequency patterns, whether due to aliasing or not.

In the following section, we show how the neural filter model can explain not only the CSF notch, but the conspicuous asymmetry in peak sensitivity between the "direct resolution" and "aliasing" CSF lobes which flank it.

B. Visibility of patterns due to aliasing: experiment and theory

The pattern threshold data conform qualitatively to the expectations outlined in the introduction to Experiment 2: the CSF for pattern sensitivity exhibits a true resolution lobe declining steeply toward the Nyquist frequency (about 60 cpd), and alongside it an aliasing lobe that appears at supra-Nyquist frequencies and peaks near the receptor mosaic sampling frequency (around 120 cpd). The aliasing lobe, however, exhibits an almost tenfold reduction in peak sensitivity relative to the true resolution lobe. A reduced sensitivity in the aliasing range is to be expected for two reasons. First, the receptor aperture is large enough to attenuate appreciably the stimulus contrast at frequencies above 100 cpd [13]. This factor by itself would reduce the aliasing sensitivity at the peak of the aliasing lobe to roughly half of the peak sensitivity for true resolution in the sub-Nyquist range, but a roughly fivefold reduction of aliasing sensitivity remains to be accounted for. The second factor is the dispersion of aliased energy due to the randomness of the receptor mosaic [17]. We can evaluate the effect of this quantitatively by developing a simplified model of the detection of aliased patterns.

The foveal mosaic, though locally fairly regular, exhibits some variability in intercone distance and also varies in its local hexagonal submosaic orientation from one small neighborhood to another [22]. Because of the randomly varying local orientation of the mosaic, the power spectrum of an extended patch of foveal retina is the sum of randomly oriented submosaic spectra. In this way the 6 points that surround the DC component at the origin in the power spectrum of a hexagonal mosaic are replaced by a ring (see Figure 11a, the central ring), within which their power is dispersed more or less uniformly over all orientations. Because of the slight variation in intercone distance, this ring has non-negligible width: Yellott's qualitative description of the power spectrum suggests that the ring's radial cross-section might be approximated by a

Gaussian with a standard deviation of roughly 20 cpd about its peak. The center-to-peak radius of the ring is given by the cone mosaic sampling frequency. In Yellott's observations the ring radius was about 125 cpd. (The higher-frequency components also present in the power spectrum of a regular mosaic are at frequencies at least √3 higher, and for that reason alone are unlikely to be a factor in our experiments. They were in any case not conspicuous in Yellott's observations of the spectrum produced by an array of pinholes at the cone locations; presumably jitter in the cone locations averages these higher frequencies out. In the case of the actual retina they are further reduced by spatial integration within the receptor aperture.)

Aliasing of a sinusoidal grating at or close to the ring radius frequency generates a "ring of power" centered on the stimulus frequency and hence passing through or close to the origin (Figure 11a), since under reasonable simplifying assumptions, in the limit of large array size (Yellott, personal communication) the power spectrum of the sampled stimulus is the power spectrum of the incident intensity distribution convolved with the mosaic power spectrum[17]. (Note that this power spectrum represents not optical power, but the squared amplitudes of the Fourier components of the sampled stimulus waveform.) The aliasing ring in the mosaic spectrum has the power density distribution

$$p(f_x, f_y) = P\exp[-((f_x^2 + f_y^2)^{0.5} - f_a)^2 / 2\sigma_a^2] \quad (3)$$

where f_a, the peak frequency of the aliasing ring, is 125 cpd and σ_a, the standard deviation giving the width of the ring, is 20 cpd.

The total power in the ring, which is reflected in the constant P, is not known from Yellott's optical observations, but it can be approximately determined *a priori*. If the DC power is taken as the unit, the total power in the ring (neglecting the attenuation by the photoreceptors) should integrate to 6, since the ring incorporates the dispersed power from 6 components of the regular mosaic spectrum, each equal to the DC component. The integrated ring power can be obtained symbolically, by first expressing the power as a function of the frequency $f = (f_x^2 + f_y^2)^{0.5}$, (integrating over all orientations), and then integrating with respect to *f*:

$$\int_{-\infty}^{\infty} 2\pi f \exp[-(f - f_a)^2 / 2\sigma_a^2]df$$

$$= \int_{-\infty}^{\infty} 2\pi f_a \exp[-(f - f_a)^2 / 2\sigma_a^2]df + \int_{-\infty}^{\infty} 2\pi (f - f_a) \exp[-(f - f_a)^2 / 2\sigma_a^2]df$$

$$= (2\pi)^{3/2} f_a \sigma_a \quad (4)$$

since the second integrand has odd symmetry and integrates to zero. For an integral of 6, the constant *P* in Equ. (3) and below must then have the value

$$P = 6 / ((2\pi)^{3/2} f_a \sigma_a) \quad (5)$$

Yellott's[14] convolution principle implies that the "ring of power" for a vertical sine wave grating stimulus of (horizontal) frequency f_S and contrast *c* has the density distribution obtained by displacing the mosaic power density horizontally by f_S and multiplying it by the stimulus power (the square of the contrast):

$$p_s(f_s, f_x, f_y) = c^2 p(f_s - f_x, f_y) \quad (6)$$

If f_S is close to f_X, the low-frequency components of the sampled stimulus will include part of this ring as well as the DC component of the stimulus at the origin (Figure 11a). The effective stimulus contrast is reduced, as previously mentioned, by attenuation due to spatial integration within the photoreceptor aperture. To quantify this, we adopt MacLeod et al's [13] Gaussian characterization of the spatial frequency response of the cone photoreceptors for interference fringe patterns. They did not state the standard deviation of the Gaussian, giving instead the full width at half height of the corresponding point spread function. That value averaged for their three observers was 13.5 seconds of arc of visual angle, which corresponds to a point spread function standard deviation of 5.73 seconds of arc, or 0.00159 degrees. The line spread function is in this case the same as the point spread function. The standard deviation (σ_c in the equation below) of the corresponding Gaussian ($\exp[-(f_S^2)/\sigma_c^2]$) that describes the effective contrast of an interference fringe pattern as a function of its spatial frequency (the Fourier transform of the line spread function), is $(1/0.00159)/2\pi$ cpd, or 100 cpd. The effective contrast of the stimulus is multiplied by this contrast attenuation factor, and the power density distribution is multiplied by its square. Thus, letting *c* now denote the stimulus contrast prior to spatial integration across the photoreceptor apertures:

$$p_s(f_s, f_x, f_y) = c^2 p(f_s - f_x, f_y) \exp[-(f_s^2) / \sigma_c^2]$$

$$= c^2 P \exp[-(((f_s - f_x)^2 + f_y^2)^{0.5} - f_a)^2 / 2\sigma_a^2 - f_s^2 / \sigma_c^2] \quad (7)$$

where σ_c = 100 cpd.

Sensitivity to the aliased pattern depends not only on its power distribution but on the visual system's sensitivity to

the different spatial frequency components in the pattern. The data of Koenderink and van Doorn [18] on visibility of narrow bandwidth spatial random noise patterns show that only a narrow range of spatial frequency components are efficiently detected in a noise stimulus: at high luminance levels, threshold r.m.s. contrast at a center frequency f cpd varies very roughly as $0.005(1+2f)$. If we make the simple assumption, for which there is some experimental support[23] that detectability of a complex stimulus depends on the integrated power (the squared contrast) of its frequency components, weighted by visibility--an assumption which requires in this instance that the region of spatial integration at threshold be large enough to span many differently oriented submosaics--then the threshold contrast c must be such that the integral of the power, weighted by $(1+2f)^2$ is equal to $(0.005)^2$. Thus at threshold, the stimulus contrast c must satisfy

$$c^2 \iint P \exp[-(((f_a - f_x)^2 + f_y^2)^{0.5} - f_a)^2 / 2\sigma_a^2 - f_s^2 / \sigma_c^2][1 + 2((f_x^2 + f_y^2)^{0.5})]^2 df_x df_y = 0.000025 \quad (8)$$

The dashed curve in Figure 10 shows contrast sensitivity computed as 1/c in Equ. (8) with no free parameters. The shape, width, horizontal position and height of this theoretical aliasing sensitivity curve agree roughly with the experimental data (Height and width are slightly better matched with σ_a = 15 cpd, a value also consistent with Yellott's qualitative description of the mosaic spectrum; horizontal position shows a discrepancy that is within the likely range of individual differences in the scale of the mosaic [24]. These calculations bear out our initial assumption (in the Introduction) that aliasing is not an effective cue for detection in the frequency range just above the resolution limit. They also predict correctly that alias sensitivity is poor at best, mainly because even with the comparatively regular foveal cone mosaic, the dispersion of the aliased energy over all the orientations represented within the ring of power means that only a small fraction of that energy is low enough in frequency to be useful for detection, namely the fraction that falls within Koenderink and van Doorn's relatively small window of visibility in the frequency domain and hence can be transmitted by the relevant neural filters.

As Figure 10 shows, the predicted sensitivity in the aliasing range actually falls a little below what we observed. This could be the result of our simplifying assumption that the ring of power is effectively uniform. As noted, this is justified only if the region of spatial integration for pattern detection spans differently oriented submosaics. In reality, different submosaics are certainly processed somewhat independently, as suggested by the local variations in the orientation of the zebra stripes. A more exact model of aliasing sensitivity, accommodating this fact, would require both knowledge of the two-dimensional range of neural spatial integration and a statistical model of the retinal mosaic.

Nevertheless, the above analysis suggests that even in the fovea, visibility of aliasing with grating stimuli may be somewhat restricted by the irregularity of the cone mosaic, in the way suggested by Yellott [17] for extrafoveal vision. Whether this confers any significant advantage in natural vision is doubtful: irregularity brings no advantage for spatially random stimuli, and in the natural environment grating stimuli are rare, although edges and periodic textures are ubiquitous.

Another lesson from this analysis, and from the observations of Figure 10, is that aliasing in the fovea is not a serious enough threat to vision to serve as an important constraint on the design of the eye. In order to avoid visible aliasing, it is enough that the contrast of the retinal image decline by a factor of 2 at a spatial frequency of roughly 80 cpd (adjustment thresholds of SH) or 100 cpd (calculations from Yellott's physical data [17]). The eye's optical passband is distinctly less than this [25], so avoidance of aliasing is probably not an important evolutionary constraint limiting the optical passband.

C. The appearance of a sustained fringe pattern near the resolution limit

Experiment 2 supports a model in which the notch that separates the domains of aliasing and of direct resolution is bridged by unpatterned cues to the presence of a patterned stimulus. We now turn to a discussion of the subjective character and mechanistic origin of those unpatterned cues.

A fringe pattern continuously presented at high contrast around the resolution limit appears to be randomly flickering, with enhanced brightness, and very desaturated in color[2, 3].

As we discuss elsewhere [6], our visual system has a local nonlinearity that could explain why a contrast-modulated fringe pattern may exhibit uniform flicker even when the fringe pattern is not subjectively resolved as such. This could also be the basis for the flicker seen during sustained presentation of a fringe pattern. To account for the latter we need only invoke the known involuntary eye movements during fixation, which cause a modulation of retinal illuminance at a frequency proportional to eye velocity. If the input to the nonlinear element is subject to temporal filtering, the fine fringe patterns will be effectively obliterated when the eye moves quickly, but not when it moves slowly. What we have elsewhere referred to as contrast-modulation flicker [6] will result, just as if the optical contrast of the fringe pattern had been varying [26].

Not all of the phenomena seen during presentation of a fringe pattern are explainable by local compressive nonlinearity. Notably, a sustained fringe pattern actually appears *brighter* than a uniform field of the same space-average luminance, as well as different in color [2]. Correspondingly, as we report elsewhere [6], for slow (below 4 Hz) modulation of fringe pattern contrast, the nulling luminance modulation is inverted in phase, relative to what we have reported for rapid modulation [6]. An account of this phenomenon demands a more elaborate model of the visual process than that of Figure 2. One possibility is that the increased brightness is secondary to the flicker

generated by eye movements during inspection of the fringe: it could be simply an example of the brightness enhancement associated with visible flicker [27]. But our informal impression is that the brightness enhancement associated with a subjectively comparable amount of uniform flicker is not as great as is experienced with a fringe pattern, and this suggests that spatial as well as temporal factors may contribute to it. Perhaps, for instance, brightness and color of relatively sustained stimuli are encoded by a system incorporating a rectification-like (positively accelerated) threshold nonlinearity in its response to local contrast (a reasonable assumption since this is the prototypical behavior of retinal ganglion cells). The fringe pattern will be a better stimulus to such neurons than a uniform field, even if there is a compressive transformation of luminance at its input. This could be the basis of the brightness enhancement. As to the color change, we know that independent compression of each cone's response to luminance can give a good account of the desaturation and hue shifts that occur when colors are increased in intensity [28, 29], but the desaturation of fringe patterns seems too pronounced to be explainable for on this basis with only a factor of two increase in peak luminance. It could instead be due to nonlinear compression in *contrast-sensitive* cells, making the response in M cone and L cone driven contrast-encoding cells roughly equal (since both are stimulated at high effective contrast). This requires that the contrast-sensitive cells in question be capable of resolving fringe patterns that are not resolvable subjectively. The midget ganglion cells[30,31] and LGN P cells[32] may fulfill this requirement .

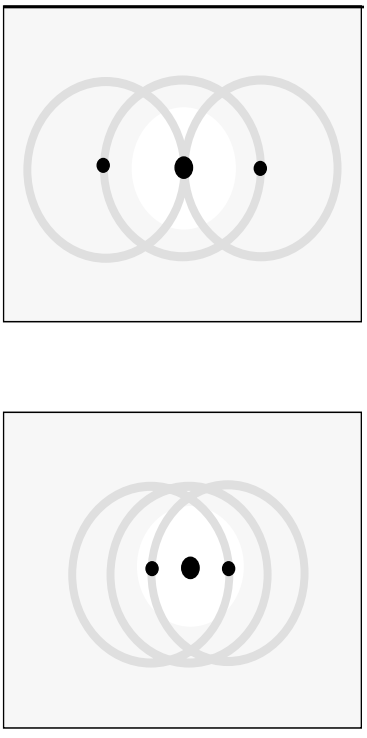

Figure 11. Power spectra of gratings sampled by a receptor mosaic. a. a vertical fringe pattern at the sampling frequency, or twice the Nyquist frequency. b. a vertical fringe pattern at the Nyquist frequency.

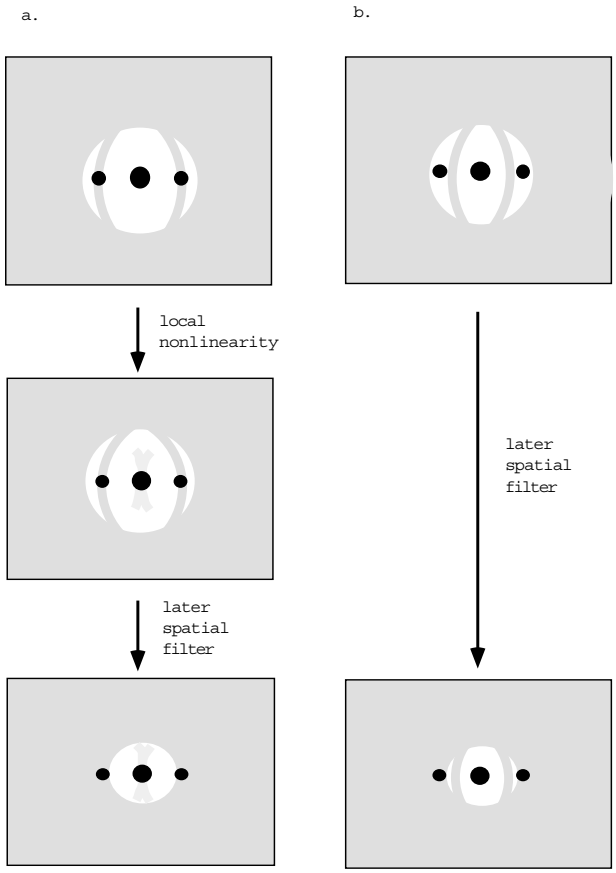

Figure 12. Power spectra of gratings sampled by a receptor mosaic. a. a vertical grating at the Nyquist frequency; the output (lower panels) contains energy preferentially at orthogonal orientation due to aliasing combined with local nonlinearity. b. a vertical grating slightly higher than the Nyquist frequency. The top and bottom panels show different sizes of the "visibility window", or bandwidths of lowpass neural spatial filter.

We have mentioned earlier that with fringe pattern frequencies close to the Nyquist frequency (about 50-70 cpd in the central fovea), a unstable structure centered around fixation can be seen, which has been described by Sekiguchi et al.[12] as "secondary zebra stripes". They have convincingly shown that this is due to aliasing in conjunction with local luminance nonlinearity. To observer SH, this pattern is restricted to a roughly 0.8x0.4 deg ellipsoid area, with the long axis lying horizontally. This area is substantially brighter than the surrounding area, and more desaturated. The vague striations inside this region seems wavy and not distinct, but they run mainly perpendicular to the original grating. Coletta and Williams [10] reported an "orientation reversal" effect in extrafoveal retina, that is, the primary aliasing pattern appeared to be at 90 degrees relative to the original grating pattern when the grating frequency was twice the Nyquist frequency at that retinal location. Figure 11a adopted from

Figure 5 in Coletta and Williams [10] explains why the secondary zebra stripes might likewise take a predominant orientation orthogonal to the stimulus stripes. The power spectrum of a sampled vertical fringe pattern at a frequency matched to the retinal mosaic (twice the Nyquist frequency) is shown in Figure 11a. The delta function at the origin and surrounding ring represent the power spectrum of the sampling mosaic. The two delta functions at left and right (for positive and negative frequency) correspond to the stimulus; each has its own surrounding ring generated by the interaction with the sampling mosaic [17, 37]. The white window in the center depicts the window of visibility, or the passband of the lowpass neural spatial filter. As can be seen from Figure 11a, within the window of visibility, the predominant energy is in the perpendicular orientation to the original fringe pattern orientation, consistent with the observation that aliasing patterns for fringe patterns at twice the Nyquist frequency appear perpendicular to the original fringe patterns [10]. The slight predominance of the perpendicular orientation in the "secondary zebra stripes" could be explained in a similar way: Figure 11b shows a schematic diagram of the power spectrum of a grating at the Nyquist frequency sampled by the cone mosaic. Again the aliased stimulus pattern power is centered on the original orientation and frequency of the fringe pattern, as shown in Figure 11b and the top panel of Figure 12a, but transmission through a local nonlinear mechanism introduces distortion products, with frequencies corresponding to the vector differences between the primary grating component and its aliased components [4]. This pattern (secondary zebra stripes) is predominantly in the perpendicular orientation to the original grating, as shown in the middle panel of Figure 12a, which represents the vector difference components of lowest frequency (those nearest the origin). Interestingly, SH also sees more regular stripes outside the above discussed "secondary zebra stripes" region, and these in many cases have the same orientation as the original grating, with an apparent frequency less than the original frequency. This is most likely the aliased pattern itself. Since the Nyquist frequency for the extrafoveal retina is lower than for the central fovea, a grating at the Nyquist frequency for the central foveal cones will be above the Nyquist frequency in the extrafovea. The power spectrum of a sampled vertical fringe pattern slightly above the sampling Nyquist frequency is shown in Figure 12b, where it can be seen that the visible power is centered on the fringe pattern orientation. Williams and Coletta [38] also showed that a experienced observer can pick up orientation information from supra-Nyquist gratings in the parafovea, where receptor packing is more disordered than that in the fovea, and proposed two hypothetical ways that this orientation information can be extracted. The difference between the two hypotheses is the post receptor neural filter bandwidth, or the window size in Figure 12b, which may be big enough to pass the delta function correspond to the original grating plus some aliasing noise (the first hypothesis, top panel of Figure 12b) or smaller so that just aliasing noise, corresponding to the crescent-shaped regions on the frequency plane, can be passed (second hypothesis, bottom panel of Figure 12b). SH's observation seems to support their second hypothesis due to the fact that the apparent frequency in the extrafoveal areas appears to be lower than the actual grating frequency. This is supported by the results of Koenderink and Van Doorn [18] on detectability of bandpass filtered spatial noise, which suggest a neural bandwidth of only a few cycles per degree.

D. The effectiveness of random flicker masking for different spatial frequencies

In Experiment II, the uniform luminance masking experiment, a possible alternative interpretation of the difference in masking effect across spatial frequency is that it might be due to the different temporal properties of different spatial frequency channels. Although temporal characteristics do vary in low and high spatial frequency channels, Breitmeyer, Levi, and Harwerth [39] found that uniform flicker can selectively mask gratings with spatial frequencies lower than about 8 cpd, but has little effect on detection of higher spatial frequency gratings. This makes it unlikely that differences in the temporal properties of different spatial frequency channels could be responsible for the selective masking effect at and above the resolution limit in our experiment. Nor could such a hypothesis explain why the masking increases rather than decreases with increasing spatial frequency near the Nyquist frequency.

To summarize, our experiments support three conclusions: (1) resolution losses of neural origin impose a resolution of about 60 cpd for fringe patterns; (2) fine interference fringe patterns at or not too far above the resolution limit are detected by nonlinear distortion products, which are spatially unstructured; (3) at spatial frequencies greater than 70-80 cpd, aliasing rather than nonlinear distortion products becomes the critical detection cue for at least some observers (although for other observers, spatially unstructured cues may remain more detectable than the aliased "zebra stripes" even at these higher fringe pattern frequencies).

ACKNOWLEDGMENTS

Pierre Durand is thanked for the many hours he spent as observer. We also want to thank Drs. Harvey Smallman, Walter Makous and Larry Thibos for their comments and suggestions on an earlier draft of this paper. Supported by NIH grant EY01711.

*Present address: Department of Psychology, Harvard University, 33 Kirkland Street, Cambridge, MA 02138; email: sheng@wjh.harvard.edu

REFERENCES AND NOTES

1. G.M. Byram, "The physical and photochemical basis of visual resolving power. Part II. Visual acuity and the photochemistry of the retina," J. Opt. Soc. Am. **34**, 718-738 (1944).
2. F. W. Campbell, and D. G. Green, "Optical and retinal factors affecting visual resolution," Journal of Physiology, **181**, 576-593 (1965).

3. D. R. Williams, "Aliasing in human foveal vision," Vision Research, **25**, 195-205 (1985).
4. D. I. A. MacLeod, D. R. Williams, and W. Makous, "Difference frequency gratings above the resolution limit," Investigative Ophthalmology and Visual Science (Suppl.), **26**, 11, (1985).
5. W. Makous, D. R. Williams, & D. I. A. MacLeod, "Nonlinear transformation in human vision," J. Opt. Soc. Am. A, **2**, P80. (1985).
6. D. I. A. MacLeod and S. He, "Visible flicker from invisible patterns," Nature, **361**, 256-258. (1993). A full length article about this work is in preparation.
7. R. W. Ditchburn, Eye-movements and visual perception. (Oxford, England: Clarendon, 1973).
8. This was suggestted to us by D. R. Williams. Based on his observation, one piece of evidence pointing to the corneal surface is that, in his eye at least, the speckles get largest and move fastest when the point sources are focused on the cornea. Moving the eye either direction axial causes them to get smaller and move more slowly.
9. L. N. Thibos, "Optical limitations of the Maxwellian view interferometer," Applied Optics, **29**(10), 1411-19. (1990).
10. N. J. Coletta and D. R. Williams, "Psychophysical estimate of extrafoveal cone spacing," J. Opt. Soc. Am. A, **4** (8), 1503-1513. (1987).
11. N. Sekiguchi, D. Williams, and D. Brainard, "Efficiency in detection of isoluminant and isochromatic interference fringes," J. Opt. Soc. Am. A, **10**, 2118-2133 (1993).
12. N. Sekiguchi, D. Williams, and O. Packer, "Nonlinear distortion of gratings at the foveal resolution limit," Vision Research, **31**, 815-831 (1991).
13. D. I. A. MacLeod, D. R. Williams, and W. Makous, "A visual nonlinearity fed by single cones," Vision Research, **32**, 347-363 (1992).
14. A. Hughes, "The topography of vision in mammals of contrasting life style: comparative optics and retinal organization," In *Handbook of sensory physiology,* 613-756. (Springer, Berlin, 1977).
15. G. Osterberg, "Topography of the layer of rods and cones in the human retina," Acta Ophthalmology., Suppl. **6**, 1-103 (1935).
16. W. H. Miller, "Ocular optical filtering," In *Handbook of sensory physiology*. Vol. 6, H. Autrum, ed. , (Springer, Berlin, 1979).
17. J. I. Yellott, Jr. "Spectral consequences of photoreceptor sampling in the rhesus retina," Science, **221**, 382-385 (1983).
18. J. J. Koenderink, and A. J. van Doorn, "Detectability of two-dimensional band limited noise," Vision Research, **14**, 515-518 (1974).
19. L. N. Thibos, F. E. Cheney, and D. J. Walsh, "Retinal limits to the detection and resolution of gratings," J. Opt. Soc. Am. A, **4**, 1524-1527 (1987).
20. R. A. Smith and P. F. Cass, "Aliasing in the parafovea with incoherent light," J. Opt. Soc. Am. A, **4**, 1530-1534 (1987).
21. L. N. Thibos, D. L. Still, and A. Bradley, "Characterization of spatial aliasing and contrast sensitivity in peripheral vision," Vision Research, **36**, 249-258 (1996).
22. J. Hirsch and W. H. Miller, "Does cone positiontiona disorder limit near-foveal acuity?" J. Opt. Soc. Am. A, **4,** 1481-1492 (1987).
23. N. Graham, *Visual pattern analyzers*. (Oxford University Press; New York, NY, 1989).
24. C. A. Curcio, K. R. Sloan Jr, O. Packer, A. E. Hendrickson, and R. E. Kalina, "Distribution of cones in human and monkey retina: individual variability and radial asymmetry," Science, **236**, 579-582 (1987)
25. D. R. Williams, D. H. Brainard, M. J. McMahon, and R. Navarro, "Double-pass and interferometric measures of the optical quality of the eye," J. Opt. Soc. Am. A, **11**, 3123-35 (1994)
26. In principle, a second possible source for flicker seen with an unmodulated fringe pattern is a aliasing process: random variations in overall (space-average) quantum catch could result from accidental variations in the registration of the fringe pattern with the cone mosaic as the eye moves. This does not depend on any early nonlinearity in processing: the operative signals could be linear records of the time variation in total quantum catch within the receptive fields of the flicker detectors. We think this linear aliasing process is unlikely to be an important source of flicker. Owing to the randomness of the receptor mosaic, the signals generated by this aliasing process will be spatially random in their temporal phase, appearing as a counterphase modulation of the fine zebra stripes rather than as the uniform field flicker that we seem to observe. Moreover, spatial integration will make this spatially random modulation harder to see. In the limiting case of a random cone mosaic, the signal amplitude for each hypothetical flicker detector is on statistical grounds limited to $n^{-0.5}$, where n is the number of cones within the flicker detector's receptive field; n is presumably very large (>100) given that spatial integration at the flicker threshold extends over several minutes of arc even in the fovea (King-Smith and Kulikowski, 1975).
27. S. H. Bartley, "Subjective brightness in relation to flash rate and the light/dark ratio," J. Exp. Psych., **23**, 313-319 (1938)
28. J. C. Maxwell, Experiments on colour, as perceived by the eye, with remarks on colour blindness. Trans. Roy. Soc. Edinburgh, **21**, 254-264 (1855).
29. J. J. Vos, "On the merits of model making in understanding color-vision phenomena," Color Research and Applications, **7**, 69-77 (1982).
30. H. Kolb, "Anatomical pathways for color vision in the human retina," Visual Neuroscience, **7**, 61-74 (1991).
31. D. M. Dacey, "The mosaic of midget ganglion cells in the human retina," The Journal of Neuroscience. **13**, 5334-5355 (1993)
32. M. J. McMahon, M. J. M. Lankheet, P. Lennie, and D. R. Williams, "Fine structure of P-cell receptive fields in the fovea, revealed by laser interferometry," Investigative Ophthalmology and Visual Science (Suppl.), **36**, 18 (1995).
33. J. J. Kulikowski and D. J. Tolhurst, "Psychophysical evidence for sustained and transient channels in human vision," Journal of Physiology, **232**, 149-163 (1973).

34. P. E. King-Smith and J. J. Kulikowski, "Pattern and flicker detection analysed by subthreshold summation," Journal of Physiology, **249**, 519-548 (1975).
35. B. B. Lee, P. R. Matin, and A. Valberg, "Sensitivity of macaque retinal ganglion cells to chromatic and luminance flicker," Journal of Physiology, **414**, 223-243. (1989).
36. W. Merigan and T. A. Eskin, "Spatial-temporal vision of macaques with severe loss of Pb retinal ganglion cells," Vision Research, **26**, 1751-1761 (1986).
37. J. I. Yellott, Jr. "Spectral analysis of spatial sampling by photoreceptors: topological disorder prevents aliasing," Vision Research, **22**, 1205-1210. (1982).
38. D. R. Williams and N. J. Coletta, "Cone spacing and the visual resolution limit," J. Opt. Soc. Am. A, **4** , 1514-1523 (1987).
39. B. Breitmeyer, D. Levi, and R. S. Harwerth, "Flicker masking in spatial vision," Vision Research, **21**, 1377-1386 (1981).